Computer-Aided Design and Applications

http://www.cadanda.com

Design for Additive Manufacturing of Cellular Structures

Chen Chu, Greg Graf and David W. Rosen

Georgia Institute of Technology, david.rosen@me.gatech.edu

ABSTRACT

Additive Manufacturing technologies enable the fabrication of parts and devices that are geometrically complex, have graded material compositions, and can be customized. To take advantage of these capabilities, it is important to assist designers in exploring unexplored regions of design spaces. This paper explores the opportunities and challenges in design for additive manufacturing. A new computer-aided design for additive manufacturing (DFAM) method is presented that is based on the process-structure-property-behavior model common in the materials design community. Examples of cellular materials design and manufacturing are used to illustrate the DFAM method.

Keywords: Additive Manufacturing, RP, Design for Manufacture, Cellular Structures.
DOI: 10.3722/cadaps.2008.686-696

1. INTRODUCTION

1.1 Design for Additive Manufacturing

The challenge for Design For Additive Manufacturing (DFAM) is to develop new methods for exploring large, complex design spaces. This contrasts with traditional Design for Manufacturing (DFM) which deals with the understanding and application of manufacturing constraints during the product design process. That is, DFM focuses on the elimination of manufacturing difficulties and the minimization of costs. With the significant improvement of rapid prototyping, or Additive Manufacturing (AM), technologies, the opportunity arises to explore design concepts that would have never been considered due to the limitations of conventional manufacturing processes.

Several companies are now using AM technologies for production manufacturing. For example, Siemens, Phonak, Widex, and the other hearing aid manufacturers use stereolithography (SL) machines [11] to produce hearing aid shells, Align Technology uses stereolithography to fabricate molds for producing clear braces ("aligners"), and Boeing and its suppliers use selective laser sintering (SLS) to produce ducts and similar parts for F-18 fighter jets. In the first two cases, AM machines enable one-off, custom manufacturing of 10's to 100's of thousands of parts. In the last case, AM technology enables low volume manufacturing and, at least as importantly, piece part reductions to greatly simplify product assembly. More generally, the unique capabilities of AM technologies enable new opportunities for customization, very significant improvements in product performance, multi-functionality, and lower overall manufacturing costs. These unique capabilities include:

- **Shape complexity:** it is possible to build virtually any shape, lot sizes of one are practical, customized geometries are achieved readily, and shape optimization is enabled. Hierarchical multi-scale structures can be designed and fabricated as well.
- **Material complexity:** material can be processed one point, or one layer, at a time, enabling the manufacture of parts with complex material compositions and designed property gradients.

New CAD and DFM methods are needed in order to take advantage of these capabilities [16]. In our paper at CAD'07 [15], we introduced these concepts and presented a method for DFAM, with a focus on integrating manufacturability assessments with design synthesis methods. In this paper, we will emphasize design exploration methods and demonstrate their application to the design of cellular materials. Cellular materials provide many more

design variables, but those additional variables add complexity. As a result, new design, analysis, and manufacturing technologies are needed.
In our view, DFM for Additive Manufacturing (DFAM) is the:

> Synthesis of shapes, sizes, geometric mesostructures, and material compositions and microstructures to best utilize manufacturing process capabilities to achieve desired performance and other life-cycle objectives.

1.2 Cellular Materials

The concept of designed cellular materials is motivated by the desire to put material only where it is needed for a specific application. From a mechanical engineering viewpoint, a key advantage offered by cellular materials is high strength accompanied by a relatively low mass. These materials can provide good energy absorption characteristics and good thermal and acoustic insulation properties as well [9]. Cellular materials include foams, honeycombs, lattices, and similar constructions. When the characteristic lengths of the cells are in the range of 0.1 to 10 mm, we refer to these materials as mesostructured materials. Mesostructured materials that are not produced using stochastic processes (e.g. foaming) are called designed cellular materials. In this paper, we focus on designed lattice materials.
In the past 10 years, the area of lattice materials has received considerable attention due to their inherent advantages over foams in providing light, stiff, and strong materials [3]. Lattice structures tend to have geometry variations in three dimensions; some of our designs are shown in Figure 1. As pointed out in [5], the strength of foams scales as $\rho^{1.5}$, whereas lattice structure strength scales as ρ, where ρ is the volumetric density of the material. As a result, lattices with a $\rho = 0.1$ are about 3 times stronger than a typical foam. The strength differences lie in the nature of material deformation: the foam is governed by cell wall bending, while lattice elements stretch and compress. The examples in Fig. 1 utilize the octet-truss (shown on the left), but many other lattice structures have been developed and studied (e.g., kagome, Kelvin foam). We have developed methods for designing lattice mesostructure for parts [22] and have developed design-for-manufacturing rules for their fabrication in SL.

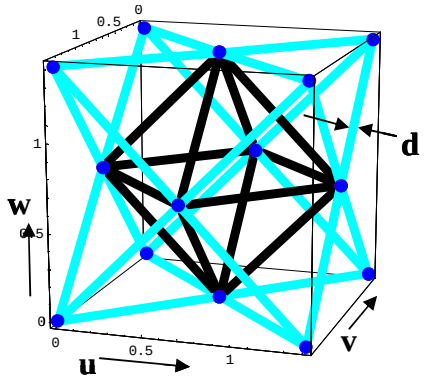

a) octet-truss

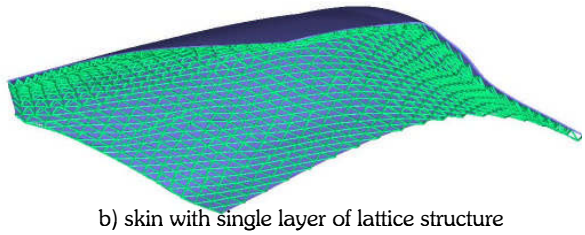

b) skin with single layer of lattice structure

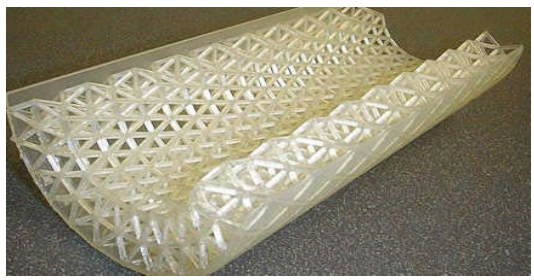

c) Skin with 2 layers of truss structure made in SL

Fig. 1: Octet-truss unit cell and example parts with octet-truss mesostructures.

Methods of continuum mechanics have been applied to various mesostructured materials. Ashby and co-workers wrote a book on metal foam design and analysis [3]. They and others have applied similar methods to the analysis of lattice structures. The octet truss in Fig. 1 has been extensively analyzed. Deshpande et al. [5] treated the octet truss unit cell as a collection of tension-compression bars that are pin-jointed at vertices and derived analytical models of their collapse behavior for many combinations of stresses. Their results match finite element model behavior well, but tend to under-predict the strength and stiffness of octet trusses due to their assumption of pin-jointed vertices. Wang and McDowell [23] extended this study to include several other lattice cells. Recently, we have been developing a more general analytical model of lattice behavior [12]. From our general model, models for octet and other lattice structures can be derived. We base our model on a single vertex with a collection of struts incident on that vertex.

1.3 Requirements for DFAM

Typically, achieving high stiffness or strength and minimal weight are typical objectives in designing parts with cellular structures. Multifunctional requirements are also common, such as structural strength and vibration absorption. The area of compliant mechanisms shares the same motivation, where the local compliance of the structure enables the mechanism to perform specified motions.

We hypothesize that designed mesostructures will enable structures and mechanisms to be designed that perform better than parts with bulk or non-designed mesostructures, particularly for multifunctional applications. Testing this hypothesis requires the ability to bridge the meso to macro size scales. To do this, we need to first recognize some requirements on DFAM methods and CAD-DFAM tools that will be developed, with a related objective of utilizing the unique capabilities of AM technologies. The requirements that we propose include the capability to:

Represent and design with hundreds of thousands of shape elements, enabling large complex design problems as well as designed material mesostructures.

Efficiently search design spaces composed of hundreds of thousands of shape elements.

Represent complex material compositions, ensure that they are physically meaningful, and determine their mechanical properties.

Ensure that specified shapes, material structures, and properties are manufacturable.

Ensure that as-manufactured designs achieve requirements.

In order to achieve these requirements, several new technologies are required. In this paper, we focus on the first two requirements above. The cellular structures under consideration here are lattice structures, which are composed of beam elements. We utilize a continuous design space defined by the sectional dimensions of these beam elements. We pursue two primary design approaches:

we develop a library of unit cells for various loading and stress-strain conditions, then place them into parts that match their load and/or stress/strain conditions. In this approach, we can avoid having to optimize the entire part design.

we utilize evolutionary algorithms to explore large design spaces. Upon identifying promising regions, conventional optimization algorithms may be applied to continue improving the design.

Both of these approaches are presented in this paper. In the next section, the formal framework for our DFAM approach is presented, providing the larger context for this research. In Section 3, the technologies being developed for DFAM are presented, with an emphasis on the development of unit cells and evolutionary algorithms. Several examples are presented in Sections 4 and 5 that cover the two design methods. Conclusions are drawn in the final section.

2. FORMAL FRAMEWORK FOR DFAM

Our DFAM framework is based upon the process-structure-property relationships from the materials science domain [14], where analysis of a material consists of examining the microstructure of the material after processing it, and determining its mechanical properties from the microstructure. In materials design, material developers seek to reverse the process by specifying desired behavior, deriving target mechanical properties, designing desired microstructures, and developing manufacturing process conditions to achieve those microstructures.

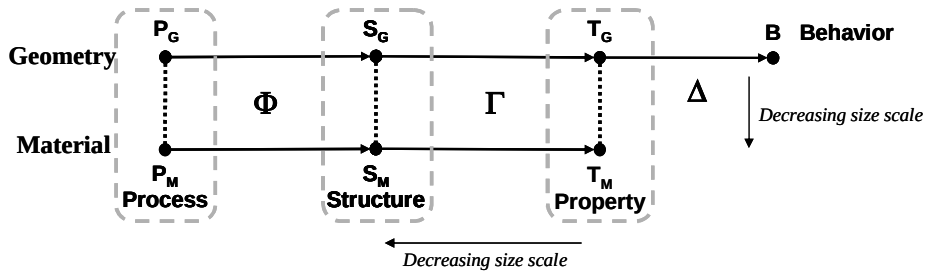

Fig. 2: DFAM Framework with Geometry and Material Layers.

In the design of cellular materials, we introduce an additional hierarchy into this framework that captures the geometric complexity of the mesostructure. As a result, part behaviors can be controlled by adjusting cellular structure geometry in addition to material microstructure. The concept is illustrated in Fig. 2. Let a solid model with material composition

and other material-related attributes be denoted as S = (*G*, *M*), where *G* is the solid geometric model and *M* is the attribute space, with some attributes being applied only to regions of G. S denotes the structure of the design. The manufacturing process space, P, consists of process plans with sequences of operations and values of process variables. Property space T contains information about part properties that are derivable from S using physical principles; e.g., mechanical, thermal, and electrical properties. Finally, we will add behavior space, B, which contains information about a part's actual and desired behavior given some loading and boundary conditions.

Mappings are defined among these spaces. Mapping Φ represents a manufacturing analysis that determines material composition and microstructure, and possibly as-manufactured part shape from a process plan. Mapping Γ represents a material science analysis of a material, and possibly part geometry, to arrive at a set of mechanical and other properties. It is possible that this mapping can be determined once, then reused for different applications.

The overall DFAM method consists of a traversal of the framework in Fig. 2 from Behavior to Process, then back again to Behavior. The traversal from Behavior to Process can be called design, where functional requirements are mapped to properties and geometry that satisfy those requirements to structures and through process planning to arrive at a potential manufacturing process. Going in the reverse direction, one can simulate the designed device and its manufacturing process to determine how well it satisfies the original requirements.

Fig. 3 shows the proposed DFAM system that embodies the framework outlined above. To the right in Fig. 3, the designer can define the DFAM synthesis problem, using an existing problem template if desired. For different problem types, different solution methods and algorithms will be available. Analysis codes, including FEA, boundary element, and specialty codes, will be integrated to determine design behavior. In the middle of Fig. 3, the heterogeneous solid modeler (HSM) is illustrated (heterogeneous denotes that material and other property information will be modeled). Libraries of materials and mesostructures enable rapid construction of design models. To the left, the manufacturing modules are shown. Both process planning and simulation modules will be included. After planning a manufacturing process, the idea is that the process will be simulated on the current design to determine the as-manufactured shapes, sizes, mesostructures, and microstructures. The as-manufactured model will then by analyzed to determine whether or not it actually meets design objectives.

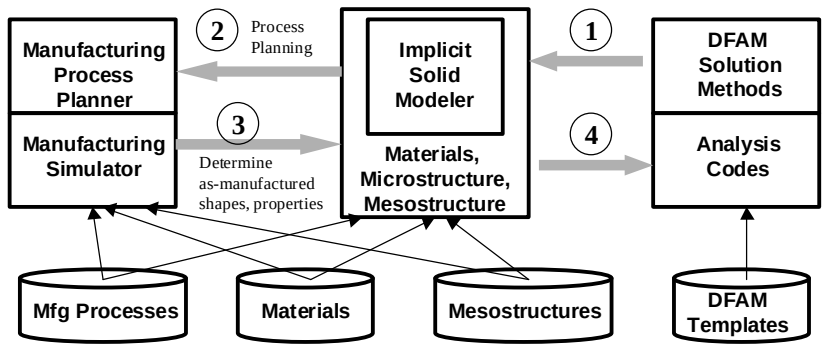

Fig. 3: DFAM System and Overall Method.

3. DFAM METHOD, SYSTEM, AND TECHNOLOGIES

3.1 CAD = Structure + Property

The CAD system proposed here consists of the Structure and Property elements of Figs. 2 and 3. Our proposed geometric representation is a combination of implicit, non-manifold, and parametric modeling, with the capability of generating BReps when needed. Implicit modeling is used to represent overall part geometry, while non-manifold modeling is used to represent shape skeletons. Parametric modeling is necessary when decomposing the overall part geometry into cellular structures; each cell type will be represented as a parametric model.

Implicit modeling has many advantages over conventional BRep, CSG, cellular decomposition, and hybrid approaches, including its conciseness, ability to model with any analytic surface models, and its avoidance of complex geometric and topological representations [6]. The primary disadvantage is that an explicit boundary representation is not maintained, making visualization and other evaluations more difficult than with some representation types. For HSM, additional advantages are apparent. Implicit modeling offers a unified approach for representing geometry, materials, and distributions of any physical quantity. A common solution method can be used to solve for material compositions, analysis results (e.g., deflections, stresses, temperatures), and for spatial decompositions if they can be

modeled as boundary value problems [20]. Furthermore, it provides a method for decomposing geometry and other properties to arbitrary resolutions which is useful for generating visualizations and manufacturing process plans.
Cellular structures are represented parametrically. The octet lattice unit cell shown in Fig. 1 includes spatial parameters *u*, *v*, *w* and size parameter *d* for strut diameters. That is, one can think of a unit cell as a primitive that can be mapped into a trivariate volume. Such primitives can be used to fill (tile) a volume that is modeled as a trivariate Bezier or B-spline volume. The mapping $\Gamma^{-1}(\mathbf{T_G}) \rightarrow \mathbf{S_G}$ is a spatial decomposition of a volume into a collection of unit cells. The decompositions of interest here are essentially mapped hexahedral meshes, with each element of the mesh consisting of an appropriate unit cell. In this manner, lattice and other cellular structures can be generated readily.
Non-manifold modeling is used to represent shape skeletons. For lattice structures, it is often sufficient to represent struts as line segments terminated by nodes. Radius parameters are associated with struts and nodes to enable reasoning about the 3D geometry of lattices and enable generation of 3D solid models, analysis models, and manufacturing models. We use a simple non-manifold model based on that of Gursoz *et al*. [10], which is particularly useful when representing lattices with skins [21]. Such models are represented by the centerlines of the lattice struts and the mid-plane of the skin (surface). Non-manifold capability enables the determination of which side of the skin the truss is on, among other reasoning tasks.

3.2 Unit Cell-Based Design Approach

The basic design concept for parts with cellular materials is as follows. Volumetric regions in the part are replaced with cells of a chosen type. Then, the entire structure is synthesized such that the dimensions of the cellular elements are sized to achieve a balance of objectives. The approach is illustrated in Fig. 4.
We have identified three types of problems of interest: minimum weight for structural applications (combination of weight, stiffness, strength), compliance distribution for applications in which a desired distribution of compliance/stiffness or other mechanical property is specified, and motion specification or mechanism design problem (compliant mechanism). Unit cell types are selected based on criteria that relate to the problem type. For example, a structural design problem would rely on criteria related to elastic modulus, strain, or stress, such that unit cell types would be selected that provide good performance relative to those criteria.

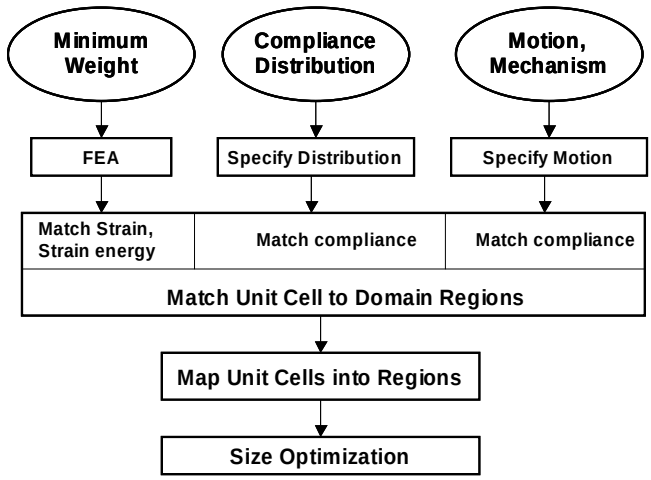

Fig. 4: Unit cell-based design synthesis approach.

3.3 Unit Cell Library

The unit cell types in our library have structure and property information. Currently, we have two 3D unit cells, the octet lattice [5] and a lattice structure that was developed to be injection moldable [4]. In 2D, we have two unit cell types, one for structural applications (with three variants for shear, bending, and compression loading conditions) and one for compliant applications. We add to the library as we characterize new types in terms of their mechanical properties.
One unit cell type will be presented in detail to illustrate the types of information in our models. The structural unit cell is shown in Fig. 5, which is characterized by loading type and magnitude. For example, this cell type's stress/strain response was recorded for shear loading under various load magnitudes. For each load magnitude, a size optimization was performed to determine the sizes of the struts in the lattice to minimize weight, while not exceeding a stress threshold. The resulting relative sizes indicate the importance of each strut in resisting the load. Furthermore, the actual sizes help to determine strut sizes for cells that are mapped into part regions. In Fig. 5b, we present the stress/strain-size properties of the structural unit cell.
Matching unit cell types to regions of a part is a two step process. First, we try to match loading and/or strain patterns. That is, we investigate the local loading conditions and strains after a finite element analysis. For example, if a small region is mostly in tension, we look for a unit cell that is good at resisting tension forces and assign that unit cell to that region. If multiple loading conditions apply, we look for a unit cell that is good for general loading conditions. Second, we compute initial strut sizes based on nodal strains from the FEA and the stress/strain-size properties of the unit cell.

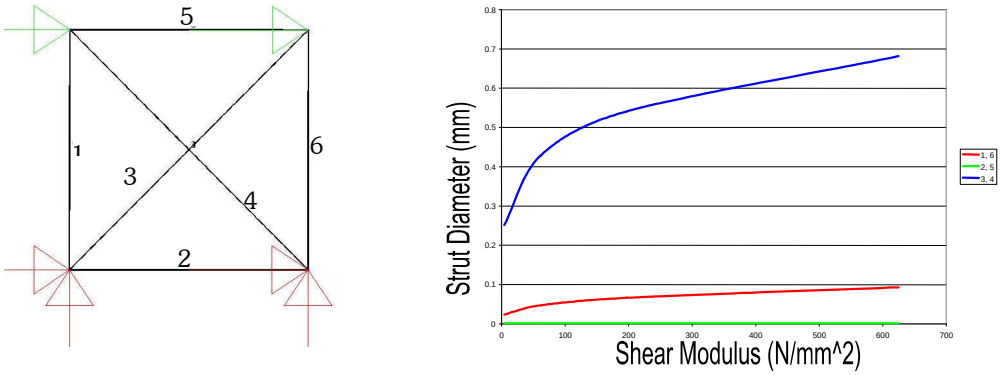

Fig. 5: 2D Structural unit cell model.

3.4 Synthesis Methods

To date, we have used a synthesis method based on Particle Swarm Optimization (PSO), which is an extension of genetic algorithms (GA), to perform parametric and limited topological optimization of structures and compliant mechanisms. PSO simulates the movement of birds in a flock, where individuals adjust their flying according to their experience and other individuals' experiences during searches for food [13]. It combines local search with global search, and enables cooperative behavior among individuals ("birds"), as well as the competition modeled using GA. Hence, PSO often converges more quickly than GA and was selected for the design synthesis of cellular structures [7].
In the future, we intend to adopt a two-stage method for multifunctional topology design applications that demand not only targeted structural performance but also satisfactory performance in a distinct secondary functional domain [18]. Intended secondary domains, such as conjugate heat transfer or vibration absorption, are governed by non-local, scale-dependent phenomena that are not directly amenable to standard homogenization or interpolation techniques underlying discrete or continuum topology optimization techniques. For this class of applications, conventional approaches involve either selecting a standard topology or identifying a final topology via conventional *structural* topology optimization and thereby fixing its topology for subsequent *multifunctional* customization. Instead, a two-stage approach for multifunctional topology design is promising in which both topology and dimensions are adjusted for multifunctional performance requirements. For the first stage, a robust structural topology design process has been developed for designing a preliminary topology with structural performance that meets targets as closely as possible while remaining relatively insensitive to bounded adjustments in the topology itself and its dimensions. In the second stage, the topology is modified, within the acceptable bounds, to improve its multifunctional performance in a secondary domain. The method relies on approximate physics-based models to facilitate rapid exploration of a broad design space and identification of promising multifunctional solutions that are verified subsequently with more detailed models.

3.5 Process Planning

Process planning is denoted by the mapping Φ^{-1}: S $\rightarrow$ P. Using the notation in Fig. 2, process planning consists of two parts, one dealing with geometry decomposition (Φ^{-1}: $S_G \rightarrow P_G$) and the other for assigning values to process variables (Φ^{-1}: $S_M \rightarrow P_M$) to process the material appropriately. The specifics of our approach were presented in earlier papers [15, 17].

4. BEAM EXAMPLE

The first of two examples consists of designing a tapered beam to achieve two different objectives. First, the beam will be designed to be as stiff and lightweight as possible. Second, the beam will be designed to have a desired distribution of compliance, as if it was to have soft and hard regions.

4.1 Structural Design Problem, Mapped Unit Cell Approach

The first beam problem focuses on the application of lattice structure's ability to provide a high stiffness-to-weight ratio. Fig. 6 shows the beam design problem, which is essentially a cantilever curved beam that is fixed on the left and free to deform in response to the downward load on the right. Our goal is to decrease the weight of the beam without significantly impacting the resulting deflection. By implementing a cellular structure approach, we are able to place

material where it will contribute most to the stiffness of the beam, and remove material where its contribution is minimal.

The design process follows that shown in Fig. 4. An initial FEA model provides strain and stress distributions that can be used to specify a range of desired elastic moduli throughout the solid body. These moduli are chosen such that the body is stiffer in areas of higher strain, and less stiff in areas of lower strain. By utilizing a suitable mesh in the FEA model, similarly sized lattice cells can be associated with one or several corresponding finite elements. This allows the selection of appropriate cell types and sizes that exhibit the desired structural characteristics, thereby placing material only where it is needed to provide the necessary stiffness. The unit cells in this example were based on the cell in Fig. 5. Variations for shear, bending, and compression loads were utilized. The resulting lattice representation of the beam contains 371 struts of circular cross section, whose diameters range from 1-5mm. The distribution of strut diameters, as shown to the right in Fig. 6, corresponds to the distribution of stresses computed in the FEA to the left. Since both the cell types and sizes reflect the strain conditions within the original beam, the lattice structure is already tailored to the characteristics of the design problem. If desired, a size optimization problem can then be completed using the calculated strut diameters as a starting point for further study. This would further refine the strut sizes to yield a stiffer and lightweight beam, while taking advantage of a greatly reduced design space defined around the calculated diameters.

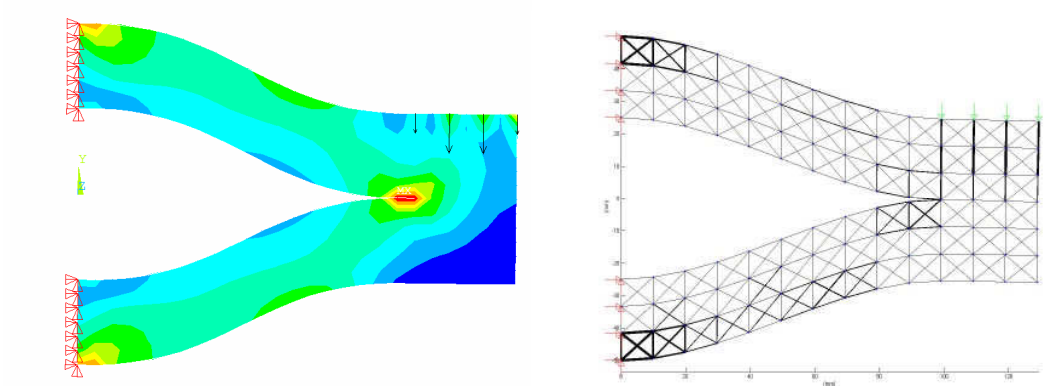

Fig. 6: FEA and truss model of first beam design problem.

4.2 Stiff + Compliant Design Problem

The second beam problem focuses on the application of cellular materials to the achievement of a desired distribution of compliance. The problem is presented in Fig. 7 for the 80 cm long beam, with symmetry assumed along the X axis. A region of "soft" compliance is desired along about 1/3 of the curved shape of the beam top, while the remainder of the structure is to be stiff. We also desire to minimize weight. In addition to compliant mechanisms, the design of integrated furniture may provide an opportunity for such design problems.

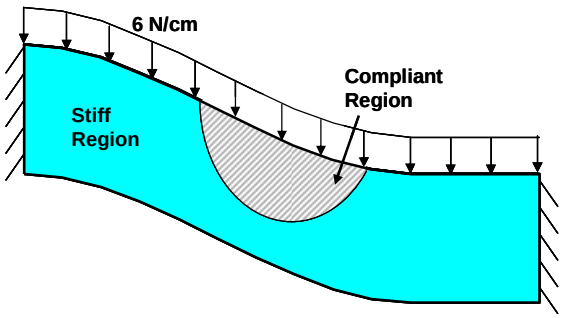

Fig. 7: Schematic of beam design problem.

To start the design process, the stiffness/compliance requirements are converted to desired displacements. For a uniform loading of 6 N/cm, the desired deflection of the stiff regions is 1 mm, while in the softer region, the desired displacement is 20 mm. Linear variation of displacements is assumed in between. With displacements specified, mesostructures can be selected. Stiff and compliant cell types are selected for their respective regions. Beam elements are assumed to have square cross-sections, with the cross-section widths as the design variables. For this problem, the model has 696 beam elements, but 596 design variables since some of the elements were constrained to have the same cross-sections. Minimum and maximum beam widths were specified as 3 mm and 6 mm, respectively. The objective function to be minimized is:

$$Z = \frac{w_d}{18}\left[\sum_{i=1}^{8}\left(y_{si}-1\right)^2 + \sum_{i=1}^{2}\left(y_{mi}-10\right)^2 + \sum_{j=1}^{8}\left(y_{cj}-20\right)^2\right] + w_V V \qquad (1)$$

which balances the deflection and volume objectives, where y_{si} are the displacements of the top nodes in the stiff region, y_{cj} are the deflections of nodes in the compliant region, y_{mj} are the deflections of nodes in the region in between, V is the part volume, and w_d and w_v are the weights for the deflection and volume objectives, respectively.
The PSO algorithm was used to solve the problem. Twenty iterations were performed with sample sizes of 220. The best result in our preliminary investigation had a deflection deviation value of 0.422 cm^2 (expression in Eqn. 1 in square brackets divided by 18 (average squared deviation)), a volume of 679.8 cm^3, and an objective function value of 0.667 for weights w_d = 0.76 and w_v = 1/2000. The final beam model is shown in Fig. 8, with strut width proportional to line thickness. Blue dots indicate nodes. The loading conditions can be seen as green arrows along the top curve, while the red symbols along both sides indicate the fixed boundary conditions. The achievement of displacement objectives can be seen in Fig. 9. The black curve indicates the actual deflection of nodes along the top curve, while the dotted blue curve indicates the desired deflection profile.

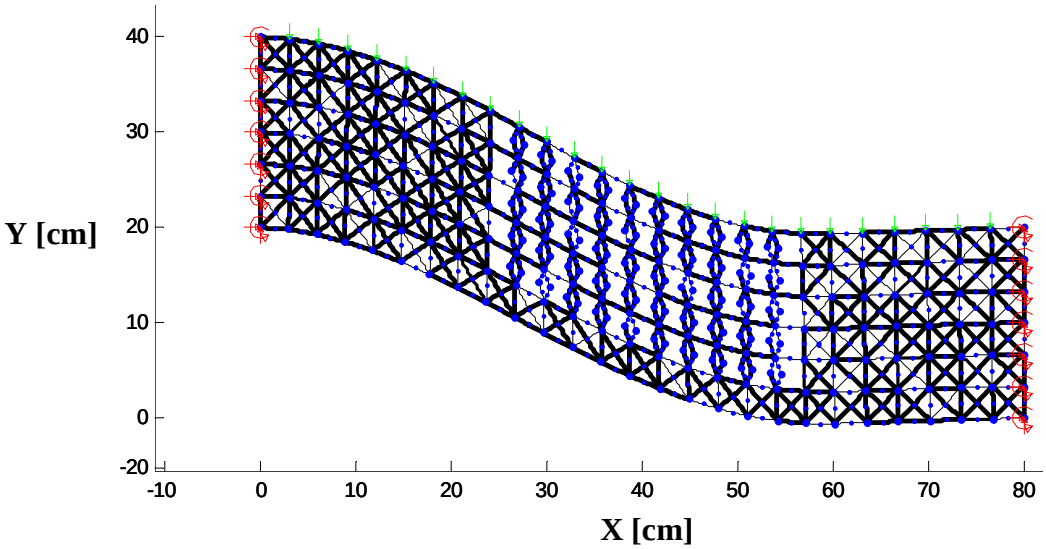

Fig. 8: Final beam design, with loading and boundary conditions.

Results correspond to expectations. Many of the struts in the stiff region were at their maximum width value of 6 mm. Thinner struts tended to be in the compliant region, although quite a few thin struts are in the "stiff" region near the right boundary in order to save weight. Given the stochastic nature of the PSO algorithm, the distribution of beam widths appears somewhat random. Of the 696 struts in the beam, 440 were at their maximum bound (0.6 mm), 90 were at their minimum bound (0.3 mm), and the remaining 66 were distributed between the bounds. Using larger populations and greater numbers of iterations may produce more uniform results. Nonetheless, the results of this PSO exercise represent a significant improvement over a nominal design with a uniform strut thickness.

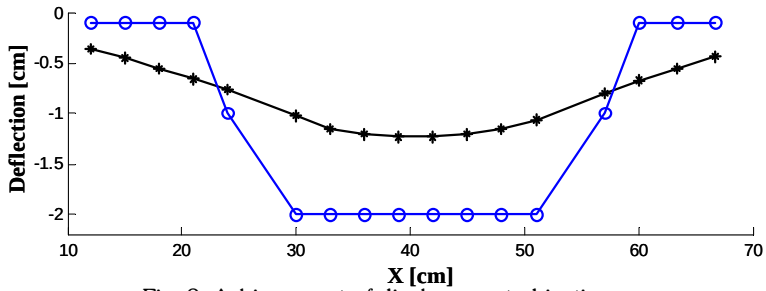

Fig. 9: Achievement of displacement objectives.

5. MORPHING AIRFOIL EXAMPLE

The aerodynamic performance of an airfoil greatly depends on the airfoil geometry. Most airplane wings are sufficiently rigid without significant movement or twist during flight. For example, large aircraft wings designed for efficient high-speed flight incorporate some form of rigid trailing edge flap and perhaps a rigid leading edge device such as a slat to achieve high aerodynamics performance. However, future airplanes may have flight controls integrated into the wing and may even fly like birds with flexible wings. Morphing wings may consist of a single element with sophisticated structures that can reconfigure their shape and adapt to changing flying conditions. As a

result, changes in the geometry of the wing might be used to control flight, suppress flutter, reduce buffeting effects, and maximize fuel economy. Morphing wings might enable the design of multifunctional aircraft.
An example problem, a morphing wing concept for AAI's Shadow [1], is proposed as an example study in this research. AAI's Shadow is a small Unmanned Aerial Vehicle (UAV) for information collection [2]. The flight range and endurance of UAVs are limited by their fuel storage capacity. It is greatly desired to increase the flight range and endurance without the addition of fuel. During a mission, as the fuel is burned, the total weight of the UAV decreases. Therefore, the wings' working condition changes, and a different airfoil shape would better serve the aircraft. In the AAI's Shadow example studied by Gano and Renaud [8], the wing cross-section morphs from the NACA 23015 airfoil to FX60-126 as shown in Fig. 10. The NACA 23015 airfoil, represented by the outer profile in Fig. 2, is bulky and has more capacity to store fuel at the beginning of the mission. The FX60-126 airfoil, represented by the shaded region, is slender and represents the shape at the end of the mission. The profile coordinates of NACA 23015 and FX60-126 airfoil cross-sections were obtained from the UIUC airfoil data site [19]. The coordinates can be scaled uniformly. The chord length of both airfoils is 300 mm.

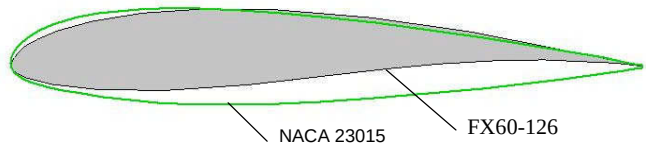

Fig. 10: Airfoil Morphing from NACA 23015 to FX60-126.

Gano and Renaud concluded that the range of the UAV with the variform wing was 22.3% farther and the endurance was 22.0% longer than the initial static NACA 23015 airfoil. They developed a morphing wing design that was actuated by the size reduction in the wing's inflatable fuel bladders. In our earlier work, we also developed a morphing wing design that was able to match the shape of the FX60-126 airfoil. In this paper, we illustrate the cellular material-based design method for the generation of a new solution to the morphing wing problem.

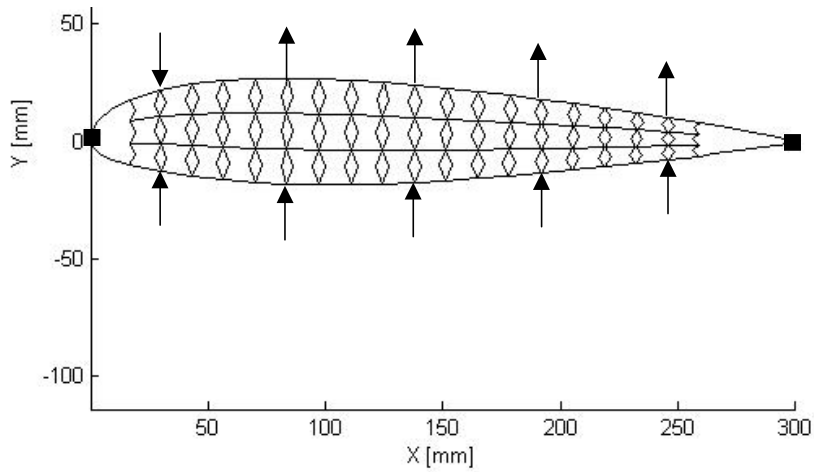

Fig. 11: Starting airfoil shape, cellular structure, and loading and boundary conditions.

Since most of the profile changes occur in the middle part of the airfoil, we chose to place cells into the middle region of the airfoil, but not at the ends, as shown in Fig. 11. Five sets of actuators were placed on the airfoil boundary to mimic the loads applied by fuel bladders emptying. The end nodes, shows as black squares, were fixed in X and Y. As in the beam example, we want the design to be light weight, but in this special case, the shape is more important. Thus we set our objective function to:

$$Z = w_d \times mean(SD_k) + w_v \times V \tag{2}$$

in which $mean(SD_k)$ is the mean squared deviation (bracketed term in Eqn. 1) between the desired shape and the actual shape under deformation among 12 sample points, V is the normalized total material volume, and the weights

are w_d = 12, w_v = 1/120000. Rectangular cross-sections were applied for each strut, with a common width of 5 mm and the height as the design variable. Upper and lower limits on the heights were 5 and 0.5 mm, respectively. Giving the trusses a uniform height of 5 mm, the mean square displacement deviation was 36.43, the volume was 62,800 mm^3, and the objective function value was 1094.
Ten iterations of the PSO algorithm were performed with sample sizes of 97. The best result obtained is shown in Fig. 12, with deviation, volume, and objective function values of 12.11, 32,500 mm^3, and 364, respectively. The optimized airfoil gets much closer to the desired streamlined airfoil shape than the starting design and weighs considerably less. The deformed airfoil requires some additional refinement to ensure it is smoother; we will include additional sample points to try to obtain a better match to the desired airfoil.

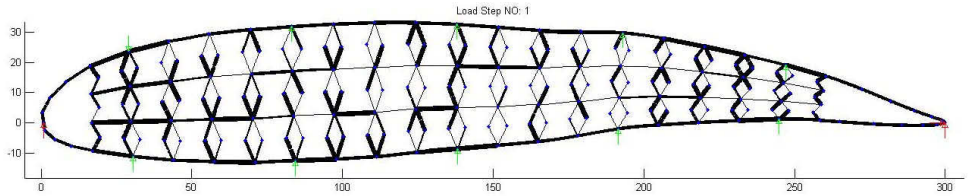

Fig. 12: Final morphing wing design in the deformed shape (airfoil FX60-126).

6. CONCLUSIONS

Two advances are reported in this paper. First, a new Design for Additive Manufacturing (DFAM) method was presented that supports part and specification modeling, design synthesis, process planning, and manufacturing simulations. Second, the efficacy was demonstrated of our unit cell approach for the initial layout of cellular structures within a part. Specific conclusions that can be drawn from this work include:

- Cellular material types provide one method for providing mesostructure within a part for achieving improved stiffness, strength, or other functional requirements, as compared to monolithic materials.
- Characterizing unit cells based on their structural performance provides useful primitives for configuring structural and compliant designs.
- The particle swarm optimization algorithm provides a useful method for exploring large design spaces; however, further investigation is needed to evaluate its efficiency and effectiveness compared with other algorithms, including genetic algorithms and other evolutionary optimization methods.
- Design for Additive Manufacturing should be concerned with the exploration of expanded design spaces, rather than the focus on constraints imposed by the manufacturing processes, as is typical of DFM methods.

7. ACKNOWLEDGEMENTS

We gratefully acknowledge the U.S. National Science Foundation, through grants DMI-0522382, and the support of the Georgia Tech Rapid Prototyping and Manufacturing Institute member companies, particularly Pratt & Whitney, for sponsoring this work. Thanks go to Dr. Hongqing Vincent Wang, of 3D Systems, for the development of the original lattice structure analysis and synthesis method used in this paper, as well as the morphing airfoil example.

8. REFERENCES

[1] Anon.: Shadow 400 UAV system, AAI Corporation http://www.aaicorp.com, September 13, 2005.
[2] Anon.: AAI RQ-7 Shadow 200, Jane's Information Group http://juav.janes.com/, September 13, 2005.
[3] Ashby, M. F.; Evans, A.; Fleck, N. A.; Gibson, L. J.; Hutchinson, J. W.; Wadley, H. N. G.: Metal Foams: A Design Guide, Butterworth-Heinemann, Woburn, MA, 2000.
[4] Cantley, R. W.: Molded Plastic Truss Work, US Patent 6,993,879.
[5] Deshpande, V. S.; Fleck, N. A.; Ashby, M. F.: Effective Properties of the Octet-Truss Lattice Material. Journal of the Mechanics and Physics of Solids, 49(8), 2001, 1747-1769.
[6] Ensz, M.; Storti, D.; Ganter, M.: Implicit Methods for Geometry Creation. International Journal of Computational Geometry Applications, 8(5-6), 1998, 509–36.
[7] Fourie, P. C.; Groenwold, A. A.: The particle swarm optimization algorithm in size and shape optimization, Structural and Multidisciplinary Optimization, 23, 2002, 259-267.

[8] Gano, S. E.; Renaud, J. E.: Optimized Unmanned Aerial Vehicle With Wing Morphing For Extended Range And Endurance, 9th AIAA/ISSMO Symposium and Exhibit on Multidisciplinary Analysis and Optimization, Atlanta, GA, September 4-6, 2002, AIAA-2002, 5668-78.

[9] Gibson, L. J.; Ashby, M. F.: Cellular Solids: Structure and Properties, Cambridge University Press, Cambridge, UK, 1997.

[10] Gursoz, E. L.; Choi, Y.; Prinz, F. B.: Vertex-based Representations of Non-manifold Boundaries, Geometric Modeling for Product Engineering, IFIP WG5.2, Rensselaerville, NY, M. J. Wozny, J. U. Turner, and K. Preiss, (eds.), North-Holland, Amsterdam, 1988, 107-130.

[11] Jacobs, P. F.: Rapid Prototyping & Manufacturing, Fundamentals of Stereolithography, SME, Dearborn, MI, 1992.

[12] Johnston, S. R.; Reed, M.; Wang, H.; Rosen, D. W.: Analysis of Mesostructure Unit Cells Comprised of Octet-truss Structures, Solid Freeform Fabrication Symposium, Austin, TX, Aug. 14-16, 2006, 421-432.

[13] Kennedy, J., Eberhart, R. C.: Particle swarm optimization, Proceedings of IEEE International Conference on Neural Networks, Piscataway, NJ, 1995, 1942-1948.

[14] Olson, G. B.: Computational Design of Hierarchically Structured Materials, Science, 277(5330), 1997, 1237-1242.

[15] Rosen, D. W.: Computer-Aided Design for Additive Manufacturing of Cellular Structures, Computer-Aided Design & Applications, 4(5), 2007, 585-594.

[16] Rosen, D. W.; Atwood, C.; Beaman, J.; Bourell, D.; Bergman, T.; Hollister, S.: Results of WTEC Additive/Subtractive Manufacturing Study of European Research, Proc. SME Rapid Prototyping & Manufacturing Conference, paper #TP04PUB211, Dearborn, MI, May 10-13, 2004. Also, see: http://wtec.org/additive/welcome.htm for the complete report.

[17] Sager, B.; Rosen, D. W.: Use of Parameter Estimation for Stereolithography Surface Finish Improvement, Rapid Prototyping Journal, accepted Feb. 2008.

[18] Seepersad, C. C.; Allen, J. K.; McDowell, D. L.; Mistree, F.: Robust Design of Cellular Materials with Topological and Dimensional Imperfections, ASME J. Mechanical Design, 128(6), 2006, 1285-1297.

[19] Selig, M.: UIUC Airfoil Coordinates Database - Version 2.0, Department of Aerospace Engineering, University of Illinois at Urbana-Champaign, Urbana, Illinois 61801 http://www.ae.uiuc.edu/m-selig/ads.html, August 10, 2005.

[20] Shapiro, V.; Tsukanov, I.: Meshfree Simulation of Deforming Domains, Computer-Aided Design, 31(7), 1999, 459-471.

[21] Wang, H.; Chen, Y.; Rosen, D. W.: A Hybrid Geometric Modeling Method for Large Scale Conformal Cellular Structures, Proc. ASME Computers and Information in Engineering Conference, paper DETC2005-85366, Long Beach, CA, Sept 24-28, 2005.

[22] Wang, H.; Rosen, D. W.: Parametric Modeling Method for Truss Structures, ASME Computers and Information in Engineering Conference, paper DETC2002/CIE-34495, Montreal, Sept. 29-Oct 2, 2002.

[23] Wang, A.-J.; McDowell, D. L.: Optimization of a metal honeycomb sandwich beam-bar subjected to torsion and bending, International Journal of Solids and Structures, 40(9), 2003, 2085-2099.